ISSN 1392-1207. MECHANIKA. Vol. 31, No. 1, 2025: 44–51

Asymmetric Helical Gears Bending Stress Calculation Formula

Xue-zhong FU*, Yu-xin JIN, Ma-long ZHAO***, Fa CAO******

*College of Mechanical and Automotive Engineering, Guangxi University of Science and Technology, Liuzhou 545616, China, E-mail: 100002350@gxust.edu.cn (Corresponding Author)

**College of Mechanical and Automotive Engineering, Guangxi University of Science and Technology, Liuzhou 545616, China, E-mail: 20220103036@stdmail.gxust.edu.cn

***Liuzhou Wuling Automobile Industry Co., Ltd., Liuzhou 545005, China, E-mail: zhaomalong@wuling.com.cn

****College of Mechanical and Automotive Engineering, Guangxi University of Science and Technology, Liuzhou 545616, China, E-mail: 202100107164@stdmail.gxust.edu.cn

https://doi.org/10.5755/j02.mech.39451

1. Introduction

With the continuous advancement of industrial technology, traditional symmetrical gear transmission systems no longer meet the demands for high performance and efficiency. New high-performance asymmetric gears demonstrate greater applicability in applications requiring high precision and reliability. The key design difference between asymmetric and traditional symmetrical gears is that the tooth profile is not symmetrical on the driving and non-driving sides. By adjusting the drive-side tooth profile angle, asymmetric gears can better distribute stress, enhance transmission efficiency, and reduce tooth surface wear particularly under high-pressure angle conditions. The bending strength at the tooth roots of both the pinion and the large gear in asymmetric gears is significantly improved compared to that of traditional symmetrical gears.

Mo et al. have established a 3D model by analysing the forming principle of the asymmetric tooth profile in internal and external helical gears, and demonstrating the advantages of asymmetric teeth. They further studied the influence of friction and shear stress on the bending stress at the tooth root[1]. Yang et al. have used the vector method to develop a numerical model of the tooth profile and demonstrated the importance of pressure angle and tooth profile parameters on the loadbearing capacity of gear teeth [2]. Umar et al. have proposed a novel method to optimize the design parameters of asymmetric gears [3]. Based on the characteristics of the involute, Bian et al. derived the equation for asymmetric spur gears with double pressure angles and analysed the relationship between contact stress and pressure angle in asymmetric gears. Asymmetric gears have superior dynamic meshing forces compared to symmetrical gears [4]. According to the geometric relation and coordinate transformation, Chen et al. derived the mathematical model of asymmetric parabolic tooth profile. This model is helpful for the design and production of asymmetric gears [5]. Zhuang et al. focused on the load carrying capacity of asymmetric gears with double pressure angles and a large pressure angle as the working side. They proposed an optimization mathematical model and obtained optimized parameters for asymmetric gears [6]. Vaghela et al. conducted parametric analysis of asymmetric gears and proposed a numerical analysis method for modelling and strength calculation of asymmetric gears. This study explores the influence of the tooth profile pressure angle on the geometric shape and meshing characteristics of the working side of the asymmetric gear [7]. Weisong's team is proposed that the increasing the pressure angle of the working tooth surface can effectively improve the wear resistance of gears [8]. Prabhu studied the correction coefficient of asymmetric tooth profile to improve the wear resistance of teeth and improve the efficiency of gears [9]. Numerous studies have shown that the bending fatigue fracture performance and contact fatigue performance of asymmetric gears surpass those of standard gears[10, 11]. Cao et al. established a precise full-tooth profile model based on the gear generation principle, providing a method for the parametric design of accurate tooth profiles [12]. Zouridaki et al. used the finite element method to analyse the influence of geometric characteristics on the bending stress and strength of asymmetric gears [13]. Puneeth et al. proposed a new contact analysis boundary condition method to evaluate the contact stress of asymmetric gears [14]. Deepak et al. evaluated the difference between the results of the helical gear bending stress calculation formula and those obtained by the finite element method of the AGMA standard [15].

At present, research on asymmetric involute gears has made more in-depth results, but the research on the calculation method of tooth root bending stress of asymmetric helical gears is still relatively scarce. Due to the special tooth profile design of asymmetric gears, the traditional gear stress calculation formulas are no longer applicable. Therefore, it is urgent to develop a new calculation method for tooth root bending stress to solve this problem. In this paper, the finite element method is used to simulate the distribution of tooth root bending stress in asymmetric gears under different working conditions, and the stress variation law is analyzed. Based on the existing empirical formula for symmetric gears, the pressure angle influence coefficient of the tooth root bending stress of asymmetric gears is proposed. Combined with the regression analysis, the tooth root bending stress calculation formula suitable for asymmetric gears is further fitted. Finally, the simulation results of the tooth root bending stress of the asymmetric gear are analyzed by Workbench software. It is then compared with the calculation results of the formula to verify the accuracy and feasibility of the derived formula.

2. Asymmetric Helical Gear Tooth Surface Digital Modeling

Compared to the standard helical gear, the tooth profiles with different pressure angles are designed on both

sides of the asymmetric helical gear. Therefore, the asymmetric helical gear cutter is also designed with a double pressure angle based on the standard rack cutter. Fig. 1 is the schematic diagram of the standard rack cutter.

The coordinate system S_1 and S_2 are rigidly fixed to the rack cutter. S_3 is the auxiliary coordinate system fixed to the rack. α_{n1} and α_{n2} are the normal pressure angles of the two tooth profiles, respectively. p is pitch; s is tooth thickness; e is the slot width; a_m is the half-groove width; m_n is the normal modulus; h_{an} is the tooth root height; h_{fn} is the addendum height; O_{r1} and O_{r2} are the center of the addendum fillet; ρ is the radius of the fillet; c is the top gap; β is the helix angle. When the tool is used to process the gear, the tool and the gear are pure rolling on the pitch line, the line segments b_1c_1 and b_2c_2 process the gear tooth profile part, and the arc segments c_1d_1 and c_2d_2 process the gear transition part.

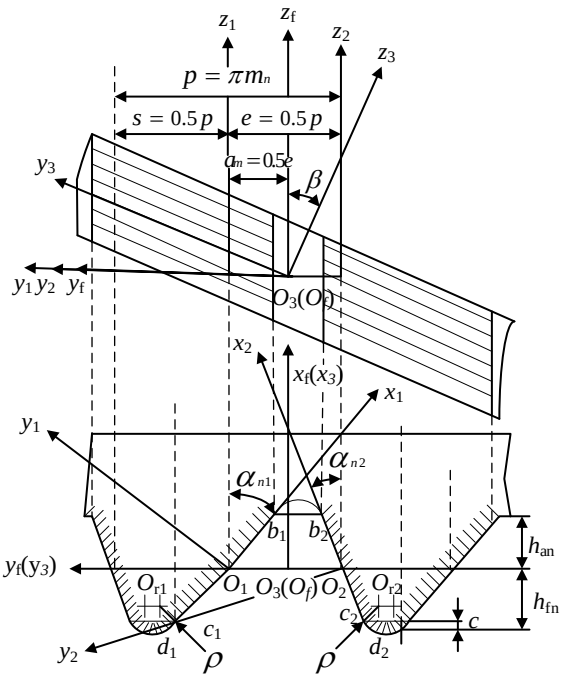

Fig. 1 Asymmetric rack cutter schematic diagram

The potential vectors of two tooth profiles $\sum b_1c_1$ and $\sum b_2c_2$ of rack cutter in coordinate system S_i (i = 1, 2) and coordinate system S_3 are

$$R_i(l_i,u_i)=\begin{bmatrix}x_i\\y_i\\z_i\\1\end{bmatrix}=\begin{bmatrix}l_i\\0\\u_i\\1\end{bmatrix}, \tag{1}$$

$$R_{3i}(l_i,u_i)=M_{3i}R_i, \tag{2}$$

where l_i and u_i (i = 1, 2) are four independent parameters of the rack cutter; u_i is the axial parameter; M_{31} and M_{32} are the 4×4 transformation matrix from coordinate system S_1, S_2 to coordinate system S_3 respectively, that is

$$M_{3i}=M_{3f}M_{fi}(i=1,2), \tag{3}$$

$$M_{f1}=\begin{bmatrix}\cos\alpha_{n1} & \sin\alpha_{n1} & 0 & 0\\ -\sin\alpha_{n1} & \cos\alpha_{n1} & 0 & 0.25p\\ 0 & 0 & 1 & 0\\ 0 & 0 & 0 & 1\end{bmatrix}, \tag{4}$$

$$M_{f2}=\begin{bmatrix}\cos\alpha_{n2} & -\sin\alpha_{n2} & 0 & 0\\ \sin\alpha_{n2} & \cos\alpha_{n2} & 0 & 0.25p\\ 0 & 0 & 1 & 0\\ 0 & 0 & 0 & 1\end{bmatrix}, \tag{5}$$

$$M_{3f}=\begin{bmatrix}1 & 0 & 0 & 0\\ 0 & \cos\beta & -\sin\beta & 0\\ 0 & \sin\beta & \cos\beta & 0\\ 0 & 0 & 0 & 1\end{bmatrix}. \tag{6}$$

The unit normal vector of the rack cutter tooth profile in the coordinate system S_3 is

$$n_{3i}(l_i,u_i)=\frac{\partial R_{3i}}{\partial l_i}\times\frac{\partial R_{3i}}{\partial u_i}\Big/\left|\frac{\partial R_{3i}}{\partial l_i}\times\frac{\partial R_{3i}}{\partial u_i}\right|. \tag{7}$$

The profile of an asymmetric involute helical gear with profile shift is enveloped by a rack cutter, as illustrated in Fig. 2. The coordinate system S_4 is rigidly attached to the asymmetric involute profile-shifted helical gear, while S_d serves as an auxiliary coordinate system. Here, θ represents the rotation angle of the gear, and $r_p\theta$ denotes the displacement of the rack cutter. r_p is the pitch circle radius of the gear, and x_n is the specified normal profile shift coefficient.

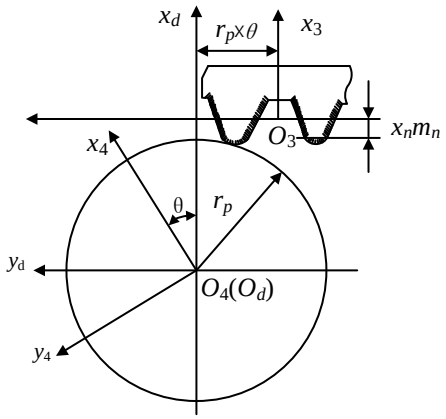

Fig. 2 Coordinate system for rack cutter and asymmetric modified helical gear generation

Therefore, the tooth surface position vector and the unit normal vector of the meshing part of the tooth profile of the asymmetric involute modified helical gear in the coordinate system S_4 are respectively

$$\begin{cases} R_{4i}(l_i,u_i,\theta,x_n)=M_{43}R_{3i}(l_i,u_i),\\ f_i=\theta-\dfrac{n_{3iy}(R_{3ix}+x_nm_n)-n_{3ix}R_{3iy}}{r_pn_{3ix}}=0, \end{cases} \tag{8}$$

$$n_{4i}(l_i,u_i,\theta,x_n)=M_{43}n_{3i}(l_i,u_i), \tag{9}$$

where f_i is the meshing equation; R_{3ix} and R_{3iy} are two coordinate components of rack cutter tooth surface normal vector n_{3i}; R_{3ix} and R_{3iy} are the two coordinate components of the rack cutter tooth surface vector R_{3i}, respectively. M_{43} is the 4×4 coordinate transformation matrix from coordinate system S_3 to coordinate system S_4, as followed

$$M_{43}=\begin{bmatrix} \cos\theta & \sin\theta & 0 & (r_p+x_n m_n)\cos\theta + r_p\theta\sin\theta \\ -\sin\theta & \cos\theta & 0 & -(r_p+x_n m_n)\cos\theta + r_p\theta\cos\theta \\ 0 & 0 & 1 & 0 \\ 0 & 0 & 0 & 1 \end{bmatrix}. \quad (10)$$

3. Calculation Method for Tooth Root Bending Stress of Asymmetric Gear

In the calculation of the bending strength of the involute helical cylindrical gear, the flat section method or the broken section method is usually used for numerical analysis. The dangerous section in the flat section method is usually cut on the tooth root transition curve formed by the tip fillet of the tool according to the 30° tangent method. However, due to the different pressure angles on both sides of the working and the non-working tooth profile of the asymmetric gear, the 30° tangent method cannot accurately determine the position of its dangerous section. Therefore, the stress concentration area in the root transition zone of the working side tooth profile is used as the dangerous section position of the asymmetric gear tooth root, and the bending strength of the tooth root is evaluated by this method.

It is assumed that the force on the gear teeth is uniform in the direction of the tooth width, so the force of the gear teeth can be simplified into a two-dimensional plane problem for analysis. Taking the end face of the gear tooth as a two-dimensional coordinate plane, the plane where the end face of the gear intersects with the center of the end face formed by the gear shaft is the center of the circle, and the connection between the midpoint of the arc of the gear tooth dividing circle and the center of the circle is set as the Y axis, and a two-dimensional rectangular coordinate system is established as shown in Fig. 3. At a certain moment during the meshing of the two gear teeth, the tooth profile is meshed at the M point. Ignoring the friction between the tooth surfaces, the gear teeth are subjected to the normal load. The action line of the force is perpendicular to the working tooth profile and intersects with the Y axis at the G point. At this moment, the load angle is the angle between the force line and the horizontal line perpendicular to the Y axis, and the load angle can be decomposed into tangential force and radial force. The tangential force produces bending stress on the dangerous section of the tooth root, and the gear is regarded as a cantilever beam with a width of b, and the dangerous section is often the key part of the failure.

According to the idea of plane section method, the dangerous section at the root of the tooth is set to AB, the bending force arm is h, the thickness of the dangerous section at the root of the tooth is, the nominal circumferential force on the end surface of the dividing circle is F, the modulus is m_n, and the pressure angle of the dividing circle on the active side is α_d, where the subscript a of the physical quantity represents the addendum circle, b represents the base circle, c represents the driven side of the gear, and d represents the active side of the gear. Through derivation, the tooth root bending stress formula of asymmetric involute helical cylindrical gear is

$$\sigma_F = \frac{F_t}{b\cdot m_n}\cdot Y_F\cdot Y_S\cdot Y_\beta\cdot Y_\alpha. \quad (11)$$

In the formula, Y_F is the tooth shape coefficient when the load acts on the external point of the single pair of teeth meshing area, Y_S is the stress correction coefficient, Y_β is the spiral angle coefficient, and Y_α is the pressure angle influence coefficient.

$$Y_F = \frac{6(h_{Fe}/m_n)\cos\alpha_{Fn}}{(s_{Fn}/m_n)2\cos\alpha_{n1}}, \quad (12)$$

$$Y_S = (1.2+0.13L)q_s^{\frac{1}{1.21+2.3/L}}, \quad (13)$$

$$Y_\beta = 1-\varepsilon_\beta\frac{\beta}{120^\circ}. \quad (14)$$

In the formula, ε_β is the longitudinal coincidence degree, L is the ratio of the thickness of the dangerous section of the tooth root to the bending force arm, $L = s_{Fn}/h$, q_s is the tooth root fillet parameter, its value is $q_s = s_{Fn}/2\rho_F$,

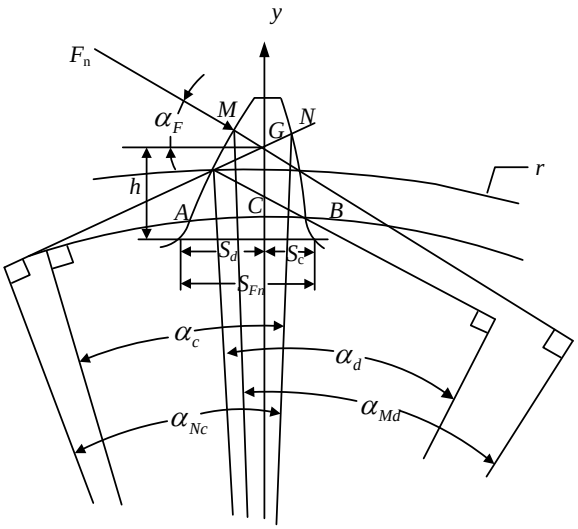

a

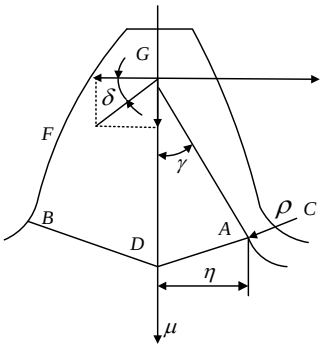

b

Fig. 3 Schematic diagram of the bending stress analysis of the tooth root: a – profile of the transverse tooth, b – dangerous section diagram of asymmetric gear

ρ_F is the curvature radius at the intersection of the dangerous section and the tooth root transition curve, α_{M1} is the involute pressure angle at the meshing point.

According to the theoretical model of the tooth root bending stress of the asymmetric gear, the program is written and the parameter values of Y_F, Y_S are obtained. At the same time, to obtain the bending stress of the asymmetric gear and the accuracy of the solution results without the finite element method, the regression analysis method is used to fit the pressure angle influence coefficient of the actual tooth root bending stress.

4. Analysis of Tooth Root Bending Stress of Asymmetric Gear

4.1. Accurate modeling and analysis of asymmetric gears

The geometric parameters of the asymmetric gear are comprehensively selected, and the key parameters such as pressure angle, addendum height and root radius of the working and non-working tooth surfaces are accurately defined in the geometric setting of MASTA, and the asymmetric gear pair model is established (Fig. 4). The material properties and boundary conditions are set, and external load conditions such as torque and speed are defined to determine the correct power flow direction in the model. In the advanced LTCA module of MASTA software, a high-precision finite element model of the gear is created according to custom mesh control (Fig. 5), and the loading contact characteristics of the asymmetric gear are evaluated in detail. based on the results of finite element analysis, the bending stress of asymmetric helical gear is obtained. The results of the analysis are shown in Table 2.

Table 2 shows that the bending stress of the tooth root increases with the increase of the working torque. Taking the working torque of 450 N·m as an example, Fig. 6 shows that the bending stress decreases with the increase of the pressure angle of the working tooth surface when the input torque of the motor is constant. The bending stress increases with the pressure angle of the non-working tooth surface.

Through analysis, it is observed that the pressure angle of the working and the non-working tooth surface, the input torque and the bending stress in the same gear interact with each other and have complicated variation rules. The

Table 1

Basic geometric parameters

Parameter	Number
Number of pinion teeth z_1	21
Number of big gear teeth z_1	53
Normal module m_n, mm	2.25
Working tooth surface pressure angle α_d, °	18-25
Non-working tooth surface pressure angle α_c, °	15-17
Helix angle β, °	28
Tooth height coefficient h_a^*	1
Dedendum coefficient h_f^*	1.25
Modification coefficient of pinion x_{n1}, mm	0.13
Modification coefficient of large gear x_{n2}, mm	- 0.13
Tooth width b, mm	30
Revolution speed n_1, r/min	3000
Torque T, N·m	150, 300, 450

Fig. 4 The gear pair model established in MASTA

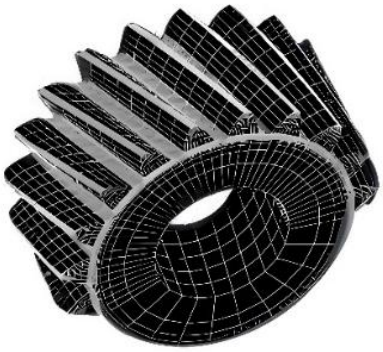

Fig. 5 Gear finite element model established in MASTA

Table 2

Bending stress results of asymmetric helical gear tooth root

Bending stress σ_F, N/mm^2	Working tooth surface pressure angle α_d, °	Non-working tooth surface pressure angle α_c, °	Input torque T, N·m
442.50	18	15	450
436.86	19		
431.47	20		
427.50	21		
424.04	22		
420.54	23		
417.07	24		
413.61	25		
304.01	18	16	300
300.12	19		
296.34	20		
292.69	21		
289.15	22		
285.73	23		
282.48	24		
280.12	25		
159.18	18	17	150
157.22	19		
155.33	20		
153.53	21		
151.81	22		
150.16	23		
148.56	24		
147.00	25		

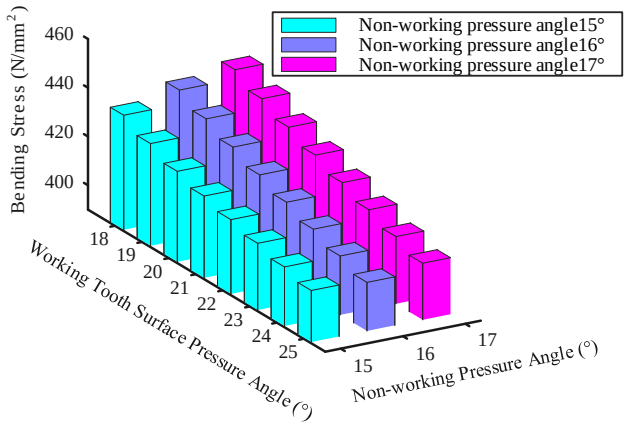

Fig. 6 Curve diagram of bending stress with pressure angle change

bending stress is linearly related to the pressure angle of the working face, the non-working pressure angle and the input torque. Based on the interaction between these parameters, the design and optimization process must consider their combined effect on bending stress. In the design, under the corresponding working conditions, the pressure angle of the working face should be maximized while reducing the pressure angle of the non-working face, while ensuring the performance and reliability of the system.

5. Calculation of Bending Stress of Asymmetric Gear Tooth Root

5.1. Bending stress solution of asymmetric gear based on regression analysis

In the article, a multivariate linear regression model is used. The basic model is as follows:

$$\hat{y}_i = \hat{\beta}_0 + \sum_{\mathrm{j}} \hat{\beta}_j x_{ij} + \varepsilon_i, i = 1,2,\cdots,n; j = 1,2,\cdots,p \quad (15)$$

where: y_i is the dependent variable; x_{ij} as independent variables; β_j is observed value, ε_i is a random error term, which is used to represent the part that the model fails to explain.

Since the curve's change trend is close to the exponential curve, the calculation formula of bending stress is set to include the form of proportional correction coefficient. At the same time, in the same pair of gears, the bending stress of the tooth root is also affected by the exponential variation law of the two parameters of the working tooth surface pressure angle and the non-working tooth surface pressure angle, as well as the combined effect of the macroscopic parameters and the microscopic parameters of the gear. Considering the influence of different pressure angles on both sides on the bending stress, the influence coefficient Y_α of the pressure angle is defined in Eq. (11). Because the curve in Fig. 6 and Fig. 7 is like the exponential curve, the mathematical expression of Y_α is defined as:

$$Y_\alpha = t_0 \frac{\theta_c^{t_1}}{\theta_d^{t_2}}, \quad (16)$$

where: Y_α is the pressure angle influence coefficient of the asymmetric helical gear, t_0 is the proportional coefficient under the change of the pressure angle when calculating the pressure angle influence coefficient. For the convenience of calculation, θ_d, θ_c is the radian corresponding to the pressure angle of the working tooth surface and the pressure angle of the non-working tooth, t_1, t_2 represents the index of the pressure angle of the working tooth surface and the pressure angle of the non-working tooth surface affected by their own changes.

According to the calculation formula of the pressure angle influence coefficient obtained by the above analysis and setting, there are three unknown parameters in Eq. (16), which are t_0, t_1, t_2. Combined with the basic mathematical knowledge, the logarithm of 10 can be taken on both sides of Eq. (16), leading to the equation shown in Eq. (17):

$$lg\, Y_\alpha = lg\, t_0 + t_1\, lg\, \theta_d - t_2\, lg\, \theta_c, \quad (17)$$

made

$$\begin{aligned} &y = lg\, Y_\alpha, b = lg\, t_0, x_1 = lg\, \theta_c, \\ &x_2 = lg\, \theta_d, m_1 = t_1, m_2 = -t_2, \end{aligned} \quad (18)$$

regression equation was gotten:

$$y = b + m_1 x_1 + m_2 x_2. \quad (19)$$

The least squares method is used to estimate the regression coefficients. The goal is to minimize the sum of squared residuals, that is:

$$Q(\beta_0, \beta_1, \ldots \beta_2) = \sum_{i=1}^{n} (y_i - \beta_0 - \beta_1 x_{i1} - \ldots - \beta_p x_{ip})^2. \quad (20)$$

According to the extreme value condition, by solving the partial derivatives and setting it to zero, a system of equations can be obtained, from which the estimated value of the coefficient can be derived. $\hat{\beta}_0$, $\hat{\beta}_1$,$\cdots$ $\hat{\beta}_p$.

$$\left[\begin{array}{l} \dfrac{\partial Q}{\partial \beta_0} = -2\sum_{i=1}^{24} (yi - b - m_1 x_1 - m_2 x_2) \\ \dfrac{\partial Q}{\partial \beta_1} = -2\sum_{i=1}^{24} (yi - b - m_1 x_1 - m_2 x_2) x_1 \\ \dfrac{\partial Q}{\partial \beta_2} = -2\sum_{i=1}^{24} (yi - b - m_1 x_1 - m_2 x_2) x_2 \end{array}\right] = 0. \quad (21)$$

Solving the above formula is attainable that $t_0 = 2.1223$, $t_1 = 0.1325$, $t_2 = -0.2404$, Therefore, using the least squares method, the empirical formula for the influence coefficient of the pressure angle considering the pressure angle of the working face and the pressure angle of the non-working face is as follows:

$$Y_\alpha = 2.1223 \frac{\theta_c^{0.1325}}{\theta_d^{-0.2404}}. \quad (21)$$

The gear macroscopic parameters, working face pressure angle, non-working face pressure angle and input torque coefficient are brought into the asymmetric helical

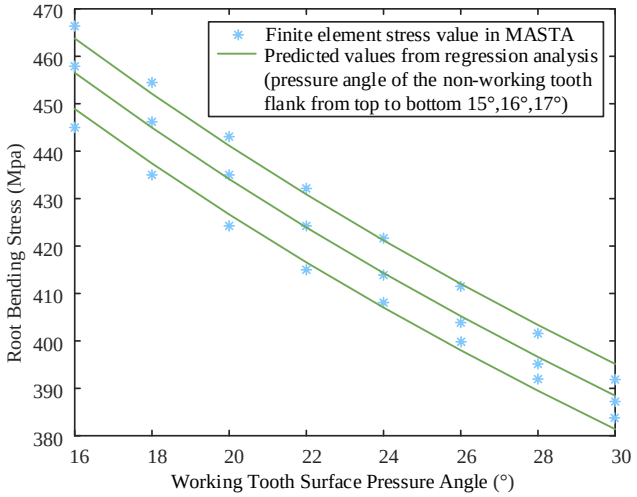

Fig. 7 The calculated value of the formula is compared with the simulation value of MASTA

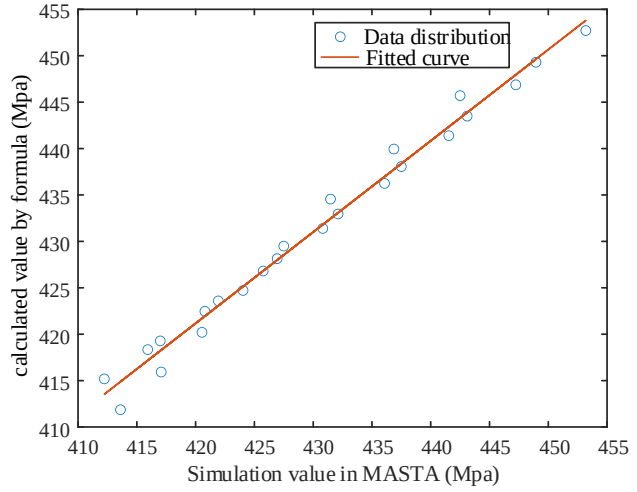

Fig. 8 The linear analysis diagram of the calculated value of the formula and the MASTA simulation value

gear tooth root bending stress Eq. (10) to obtain the theoretical calculation value of the bending stress, which is compared with the MASTA simulation value. The results are shown in Fig. 7. The simulated value of tooth root bending stress calculated under different pressure angles has obvious coincidence degree with the actual value.

The torque is set to 450 N·m, and based on this, the data samples of the pressure angles on both sides of the tooth profile are increased. Then, the theoretical calculation is carried out by using the formula method, and the bending stress is simulated and analyzed by using MATLAB software. To explore the correlation between the theoretical calculation value and the simulation value, the least square method is used for curve fitting. According to the fitting results (Fig. 8), it can be observed that there is a good linear distribution trend between the actual calculated bending stress (denoted by y) and the theoretical bending stress (denoted by x). This trend indicates that there is a significant positive correlation between the two. Through comparative analysis, the calculation results of the formula method are shown to be accurate.

6. Finite Element Comparative Analysis

6.1. Finite element example

Based on the digital tooth surface model of the asymmetric involute gear tooth profile in the previous article, the data points are calculated in MATLAB and imported into SolidWorks to establish an accurate asymmetric helical gear solid model. Based on the Workbench finite element software, the finite element analysis of the asymmetric gear model is carried out.

The established geometric model is input into the Hypermesh finite element pre-processing software, and the gear material is set as 20 CrMnTi steel material. The elastic modulus is $E = 2.06\times10^{11}$ N/m^2, the Poisson 's ratio is $v = 0.3$, and the constraint is $T = 300$ N·m. To ensure the accuracy of the model, tetrahedral elements are selected in the finite element meshing. When the gear is stressed, the tooth stress has a large gradient of stress change at the tooth root transition curve and the tooth surface. To ensure the accuracy of the stress results, mesh refinement is performed on the tooth root and tooth surface, with particular focus on further refining the tooth root region. Fig. 9 shows the mesh model of gear pair.

The gear model of the set grid is imported into the Workbench software, and the contact surface, boundary conditions and working condition parameters are set and solved. The stress distribution and displacement changes in the tooth root area under load are analyzed for different pressure angles. Simultaneously, the difference between the theoretical results obtained from the calculation formula and the simulation results is compared.

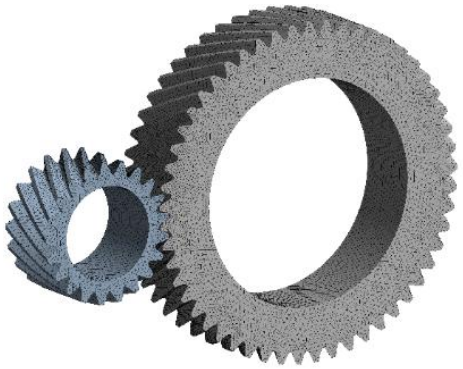

Fig. 9 Mesh Model of Asymmetric Gear Pair

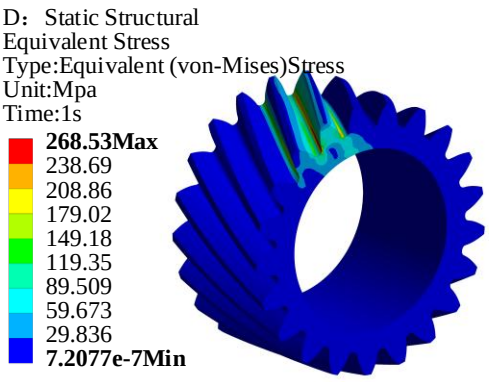

Fig. 10 Asymmetric helical gear finite element results stress cloud diagram ($\alpha_d = 25°$, $\alpha_c = 20°$)

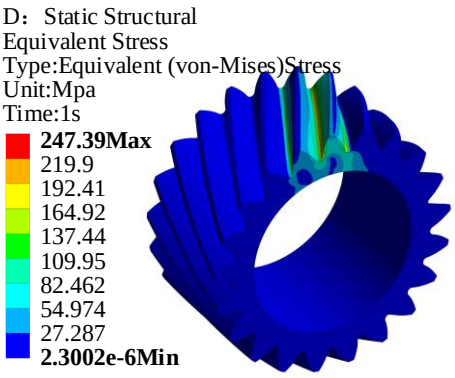

Fig. 11 Asymmetric helical gear finite element results stress cloud diagram ($\alpha_d = 30°$, $\alpha_c = 20°$)

Table 3

The results of the formula are compared with the Workbench simulation results

Asymmetric gears	Formula results	Finite element results
Bending stress ($\alpha_d = 25°$, $\alpha_c = 20°$)	282.81	268.53
bending stress ($\alpha_d = 30°$, $\alpha_c = 20°$)	260.83	247.39

By comparing the two results, the root bending stress calculated by the formula method is basically consistent with the Workbench simulation analysis results, and the error is 6.52%, which verifies the feasibility of the calculation formula of the root bending stress of the asymmetric gear.

7. Conclusions

This method is based on finite element numerical simulation and regression analysis, which can accurately predict the root bending stress under different pressure angles. By establishing the digital tooth surface model of asymmetric helical gears and using finite element software for simulation analysis, the average error rate of the calculated empirical formula is 6.52%, which proves that the derived empirical formula meets the accuracy calculation requirements. The accuracy and practicability of the derived tooth root bending stress calculation formula are verified.

In this paper, the mathematical relationship between the bending stress of the tooth root and the pressure angle of the asymmetric gear is successfully fitted by combining the stress calculation method with the regression analysis. The bending stress of the tooth root is negatively correlated with the pressure angle of the working tooth surface and positively correlated with the pressure angle of the non-working tooth surface. The results show that increasing the pressure angle of the working tooth surface and reducing the pressure angle of the non-working tooth surface can effectively improve the bending strength of the gear. The proposed empirical formula provides theoretical support and practical tools for the design of asymmetric gears, and has important guiding significance for the optimization of its bearing capacity and overall performance.

Acknowledgments

The work was supported by the Guangxi Science and Technology program (No. AD23026183), the Liuzhou Science and Technology Program (No. 2024AB0401A009), the Innovation Project of Guangxi Graduate Education (No. YCSW2024503), and the National College Students Innovation and Entrepreneurship Training Program Funding Project (No. 202310594034).

References

1. **Mo, S.; Ma, S.; Jin, G. G.; Gong, J. B.; Zhang, T.; Zhu, S. P.** 2019. Design principle and modeling method of asymmetric involute internal helical gears, Proceedings of the Institution of Mechanical Engineers, Part C: Journal of Mechanical Engineering Science 233(1): 244-255. http://dx.doi.org/10.1177/0954406218756443.
2. **Yang, Y.; Hu, J. H.; Shi, Z. Q.; Zhou, Q., G.; Wu, J.** 2024. Exact Solution of Mesh Stiffness and Analysis of Tooth Profile Parameters for Asymmetric Gear Pairs, Journal of Mechanical Transmission 48(03): 18-26. http://dx.doi.org/10.16578/j.issn.1004.2539.2024.03.003.
3. **Umar, F. N.; Parthasarathy, R.; Murshid, P. K.; Rathod, A. K.; Naveen, R. K.; Verma, A. K.; Vineesh, K. P.; Sreenath, A. M.** 2019. A Novel Methodology to Optimize Design Parameters of an Asymmetric Gear, IOP Conference Series, Materials Science and Engineering 624(1): 012016. http://dx.doi.org/10.1088/1757-899x/624/1/012016.
4. **Bian, J. Y.; Mo, S.; Han, H.; Ma, S.; Sun, Z. H.; Zhao, N. X.** 2019. Design method of asymmetrical gears and research on dynamic meshing characteristics, Journal of Machine Design 36(S1): 59-64. http://dx.doi.org/10.13841/j.cnki.jxsj.2019.s1.013.
5. **Chen, Y. J.; Yang, H. C.; Pai, P. F.** 2016. Design and kinematics evaluation of a gear pair with asymmetric parabolic teeth, Mechanism and Machine Theory 101: 140-157. https://doi.org/10.1016/j.mechmachtheory.2016.03.008.
6. **Zhuang, S. Y.; Guo, H.; Zhang, M. Q.; Sun, X. L.** 2016. FEM Stress Analysis of Spur Face Gear Pair with Asymmetric Double Pressure Angles, Journal of Donghua University (Natural Science) 42(4): 490-495. https://doi.org/10.3969/j.issn.1671-0444.2016.04.007.
7. **Vaghela, P.; Prajapati, J.** 2020. Integrated Symmetric and Asymmetric Involute Spur Gear Modelling and Manufacturing, Materials Today: Proceedings 22(4): 1911-1920. https://doi.org/10.1016/j.matpr.2020.03.091.
8. **Weisong, Y.; Shukun, W.** 2020. Wear performance of plastic gears based on asymmetric tooth profile, Journal of Mechanical & Electrical Engineering 37(5): 478-483. https://doi.org/10.3969/j.issn.1001-4551.2020.05.003.
9. **Sekar, R. P.** 2024. Reduction of tooth wear on asymmetric spur gear through profile correction factors, Australian Journal of Mechanical Engineering 22(3): 506-522. https://doi.org/10.1080/14484846.2022.2113619.
10. **Namboothiri, N. V.; Marimuthu, P.** 2022. Influence of drive side pressure angle on fracture characteristics of asymmetric spur gear, Engineering Failure Analysis 131: 105865. https://doi.org/10.1016/j.engfailanal.2021.105865.
11. **Cai, Y. J.; Yin, C. S.; Yang, L.; Liang, Z. T.; Zu, B.; Wen, Q. Y.; Hu, H. J.; Wu, Z. D.** 2022. Asymmetric

gear bending fatigue experiment contrast and analysis, Journal of Qiqihar University (Natural Science Edition) 38(5): 57-60+65. https://doi.org/10.3969/j.issn.1007-984X.2022.05.011.
12. **Cao, D. J.; Shang, P.; Cui, H. T.; Xi, W. Y.** 2023. Parametric Design of Internal Meshing Gears Based on Precise Tooth Profile Modeling, Journal of Mechanical Transmission 47(9): 66-73. https://doi.org/10.16578/j.issn.1004.2539.2023.09.010.
13. **Zouridaki, A. E.; Vasileiou, G.** 2020. Investigation of the Effect of Geometry Characteristics on Bending Stress of Asymmetric Helical Gears by Using Finite Elements Analysis, Computation 8(1): 19. https://doi.org/10.3390/computation8010019.
14. **Puneeth, M. L.; Mallesh, G.** 2021. Static contact behavior of asymmetric spur gear, Materials Today: Proceedings 47(11): 3095-3104. https://doi.org/10.1016/j.matpr.2021.06.076.
15. **Deepak, D.; Tamilselvam, P.** 2023. Theoretical and analytical research on load sharing in helical gear with evaluating the FEA method and computerized approach of AGMA standards, Journal of Combinatorial Optimization 45(3): 87. https://doi.org/10.1007/s10878-023-01003-y.

X. Z. Fu, Y. X. Jin, M. L. Zhao, F. Cao

ASYMMETRIC HELICAL GEARS BENDING STRESS CALCULATION FORMULA

S u m m a r y

Aiming at the limitation that the traditional symmetrical gear stress calculation formula cannot be applied to the new asymmetric helical gear, a calculation method of tooth root bending stress of asymmetric involute helical gear is proposed in this paper. According to the meshing principle, the digital tooth surface model of asymmetric involute helical gear is established. The distribution characteristics of tooth root bending stress are analyzed by finite element method, and the relationship between tooth root bending stress and pressure angle is studied. On this basis, the influence coefficient of pressure angle is proposed. Combined with multiple regression analysis, an analytical formula for calculating the bending stress of tooth root without finite element method is proposed. By comparing with the calculated values of the finite element method, the error rate of the theoretical formula is 6.52%, which verifies its accuracy. The research results show that the asymmetric helical gear exhibits excellent tooth root bending bearing capacity under high pressure angle conditions, which provides key theoretical support and calculation tools for the design of high-performance asymmetric gears.

Keywords: asymmetric gear, bending stress, regression analysis, pressure angle influence coefficient.

Received November 12, 2024
Accepted February 21, 2025